



Design and experimental investigation of a thermoelectric vaccine cabinet integrated with photovoltaic and nanofluids

Pinar Mert Cuce^{1,2,3}

Received: 23 March 2024 / Accepted: 3 July 2024
© The Author(s) 2024

Abstract

Vaccines are one of the most effective methods used to prevent many lethal and infectious diseases from past to present. Generally, storage temperatures of vaccines are between 2 and 8 °C. Keeping the vaccines in this temperature range and ensuring reach the end user without deterioration is very important in order to prevent the vaccines from losing their effectiveness. In this regard, various cooling systems are used. One of the devices used to ensure the cold storage of vaccines is a thermoelectric device. Thermoelectric devices attract attention as an energy-efficient technology, as well as their compact structure, silent and vibration-free operation, and suitability for automation. In this study, the design and manufacturing of a photovoltaic solar energy-driven, nanofluid-integrated thermoelectric vaccine cabinet was carried out and its performance data were experimentally examined. The capacity of the vaccine cabinet is 200 vaccine vials and 200 ready-to-use syringes, as well as the battery and inverter parts. In experiments carried out at two different outdoor temperatures, heat removal from the hot surface of the thermoelectric cooler with different refrigerants were examined. In addition, the effects of using fans were also investigated while the heat swept from the surface was transferred to the environment with the help of a water-to-air heat exchanger. In the experiments carried out for a total of 8 different cases, the highest average coefficient of performance value obtained during the experiments was 1.19. Experimental results show that vaccine storage temperatures can be reached under the prepared operating conditions.

Keywords Thermoelectric cooling · Vaccine · Coefficient of performance · Nanofluid · Cooling power

Introduction

Vaccines are one of the most important methods of preventing many diseases, such as measles, diphtheria, and tetanus, which can be lethal and contagious, especially in childhood [1]. Many deadly diseases can be prevented around the world with routine vaccination programs [2]. In addition, vaccines have played an effective way in preventing

new diseases such as COVID-19, which has threatened the whole world and caused deaths in recent years [3]. On the other hand, the economic costs of vaccines are also exceptionally high [4]. For this reason, it is extremely important that the vaccines produced can be delivered to the end user without being wasted or spoiled [5]. Except for some vaccines produced for special applications, storage conditions for vaccines are generally between 2 and 8 °C [6, 7]. For preserve and transfer vaccines cold chain tools are used in this temperature range. Cold chain is the set of special storage conditions that cover the period of keeping, storing and transporting the product at the desired temperature, from the production stage to its delivery to the end user [8]. Especially during the COVID-19 vaccination process, there were problems in shipping the vaccines to rural areas and delivering them to the end user. Therefore, the design proposed in this study targets the process of delivering vaccines without spoiling, especially from health institutions to elderly, bedridden patients in rural areas. In

✉ Pinar Mert Cuce
mertuce@gmail.com

¹ Department of Architecture, Faculty of Engineering and Architecture, Recep Tayyip Erdogan University, Zihni Derin Campus, 53100 Rize, Turkey
² Low/Zero Carbon Energy Technologies Laboratory, Faculty of Engineering and Architecture, Recep Tayyip Erdogan University, Zihni Derin Campus, 53100 Rize, Turkey
³ College of Built Environment, Faculty of Computing, Engineering and Built Environment, Birmingham City University, Birmingham B4 7XG, UK

this regard, thermoelectric devices attract attention as a clean, sustainable, and efficient technology [9].

Thermoelectric devices, which allow direct energy conversion between heat and electricity, attract attention as a promising technology to overcome global climate problems thanks to their environmentally friendly and energy-efficient structures [10]. Thermoelectric devices consist of a series of P- and N-type semiconductors. These semiconductors are connected electrically in series and thermally parallel, placed between two ceramic plates, as shown in Fig. 1. Thermoelectric devices are divided into two groups according to their operating principles: thermoelectric generators (TEG) and thermoelectric coolers (TEC) [11]. TEGs are devices that produce electrical energy from the temperature difference created between surfaces based on the Seebeck effect [12, 13]. TECs, on the other hand, work according to the Peltier effect, which is the opposite of the Seebeck effect. As a result of the electric current applied to the circuit, a temperature difference occurs between the surfaces [14].

The parameters showing the effectiveness of TECs are Figure of merit (ZT), cooling power (Q_c) and coefficient of performance (COP) values. ZT value is a measure of the usability of thermoelectric materials, and high ZT values represent high capacity. Q_c represents the cooling power obtained from the cold side of TEC. Q_c increases as the temperature difference between hot and cold surfaces decreases. The COP value represents the efficiency of TEC, and as the COP value increases, the efficiency of the system increases [15, 16]. Still, compared to traditional cooling technologies, TECs have significant advantages such as silent and vibration-free operation, long life, and low maintenance costs [17]. It offers solutions to problems such as large space requirements, mass, and transportation difficulties that are required by traditional vapor compression cooling systems [18]. Thanks to these superior features, they are used in a wide range of areas, from electronic cooling to mini refrigerators [19]. However, new designs are still being developed to increase the performance of TECs. In this regard, one of the most effective methods is the use of additional systems that reduce the hot surface temperature

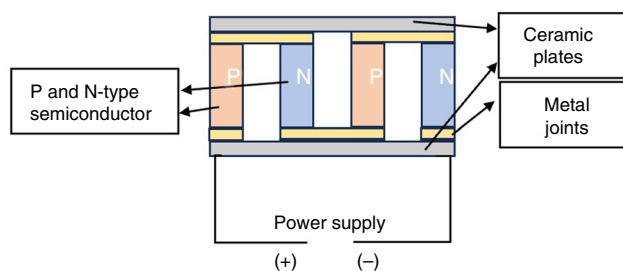


Fig. 1 Schematic description of thermoelectric devices

of the TEC [20]. Generally, aluminum heatsinks, and fans are used on the hot and cold surfaces of TEC. However, the COP values of these systems are below 0.5 [21–23]. Therefore, new methods have been developed to increase the performance of TECs. Especially keeping the hot surface temperature at low values is an effective method to increase the Q_c values of TECs [24]. For this purpose, liquid-cooled blocks are used on the hot surfaces of TECs. Water is generally used as the refrigerant, and significant improvements are achieved in the cooling performance of TECs [25]. Huang et al. [26] carried out an experimental and theoretical study to investigate the thermal performance of a TEC integrated with water cooling. The developed model has been validated with experimental data. The results obtained from the study show that the water-cooled TEC system increases the cooling performance. Hu et al. [27] experimentally examined the cooling performance of water-cooled TECs. In the study carried out for different operating conditions and environmental temperatures, two temperature controls were presented, and their performances were compared. The COP value of the proposed system in the study was observed to be approximately 0.65. Gokcek and Sahin [28] investigated the performance of a water-cooled thermoelectric refrigeration system. Different fluid flow rates and voltage values were investigated in the study where a mini channel water cooling system was used on the hot side of the TEC mechanism and heatsinks were used on the cold side. The results obtained from the experimental study show that the COP value of the system is 0.41 at a flow rate of 1.5 L/min under an 8V voltage value. In addition to increasing system efficiency by using liquid-cooled systems, heat transfer effects can be increased by using various nanofluids instead of pure fluid in these systems [29–31]. Fluids obtained by suspending nano-sized metallic or non-metallic small solid particles in a base fluid are called nanofluids [32]. Nanofluids have higher thermal conductivity values compared to the base fluid from which they are produced [33]. Due to these properties, nanofluids are also preferred in thermoelectric cooling applications. Cuce et al. [34] carried out an experimental study to investigate the effect of refrigerant use on energy efficiency in thermoelectric refrigerator applications. In the study, a water-cooled block was used on the hot surface of the TEC, and base water and different nanofluids prepared in various concentrations were tested from this block as the cooling fluid. The results obtained from the study showed that if Al_2O_3 -Water nanofluid is used as a refrigerant at a mixture ratio of 1% by mass instead of base water, it is possible to achieve an improvement of up to 26% in the initial and final temperature difference of the refrigerator cabin. In another study [35] carried out as a continuation of this study, various hybrid nanofluids were used as coolants and their effects on basic performance parameters were investigated.

It was observed that a 30% improvement was achieved for the same value when a hybrid nanofluid was used. In addition, in the best case, the COP value of the system was determined as 0.57. In another study, [36] the effect of using nanofluids on electricity consumption in thermoelectric refrigerator applications was investigated. According to the results obtained from the study, the electrical consumption values of the TEC refrigerator can be reduced by up to 50% if Al_2O_3 -Water nanofluid is used. Some other studies investigating the use of nanofluids in TEC refrigeration applications are summarized in Table 1.

In this study, the design, production, and performance analysis of a thermoelectric vaccine cabinet integrated with PVs and nanofluids, were examined. The effect of using water and nanofluids as coolants on the hot surface of TEC on the cooling performance of thermoelectric vaccine cabinets was investigated. In the vaccine cabinet produced for this purpose, water and nanofluid were circulated on the hot surface of the TEC and experiments were carried out under various outdoor conditions. Thanks to the photovoltaic (PV) panel placed on the vaccine cabinet, part of the required electrical energy can be met from solar energy and stored with a battery placed in the cabinet. During the experiments, vaccine cabinet temperatures were observed, and performance data were determined. The production steps, materials used, and experimental procedures are described in detail in the next section. In the Results section, the data obtained from the study are presented. The use of water and nanofluids as coolants on the hot surface of TEC is one of the innovative aspects of the study. Thus, it is aimed to ensure that the internal temperature of the vaccine cabinet reaches the vaccine storage temperature range earlier, thereby reducing electrical consumption values, contributing to the efficient use of energy resources, and therefore reducing carbon emissions. In all experiments carried out under 13°C outdoor conditions, vaccine temperatures reached vaccine storage conditions. In addition, thanks to

the PV panel and battery placed on the cabinet, part of the required energy can be met from renewable energy sources.

Experimental setup

Material

XPS (extruded polystyrene) insulation material was used as the vaccine cabinet. 6 mm was chosen as the insulation thickness. Since the vaccine cabinet is designed especially for portable applications, its internal dimensions were preferred as 200 mm deep, 300 mm wide and 200 mm height. These dimensions allow the placement of 200 vaccine vials and 200 ready-to-use syringes, as well as the battery and inverter parts. The view of the inside of the vaccine cabinet is presented in Fig. 2.

A monocrystalline PV panel measuring $200\text{ mm} \times 250\text{ mm}$ was used on the upper part of the vaccine cabinet. The electrical power production values of a panel with these features are in the range of 10–20 W [43]. This value can be increased if a larger PV panel is used in accordance with the dimensions of the vaccine cabinet. Therefore, some of the

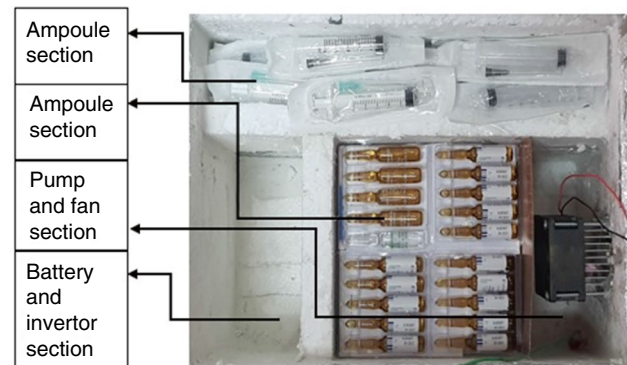


Fig. 2 The inside view of the vaccine cabinet

Table 1 The use of nanofluids in TEC refrigeration applications

Nanofluid	Concentration ratio (%)	Findings	References
Fe_3O_4 ferrofluid	0.005, 0.015	The maximum heat transfer rate is 12.57% higher than the use of water when Fe_3O_4 ferrofluid is used.	[37]
Al_2O_3 -water, TiO_2 -water	0.5 and 1	Higher thermal performance was achieved in all cases where nanofluids were used.	[38]
Al_2O_3 -water	0.1 and 0.2	A 9.15% decrease in the temperature difference between the hot and cold surfaces of the TEC was observed.	[39]
Fe_3O_4 Nanofluid	–	The performance of TEC could be increased	[40]
Al_2O_3 -water	0 to 2	The temperature difference between the hot and cold surfaces of the TEC could be significantly decreased.	[41]
CuO-Water	0.02	The convective heat transfer ratio could be significantly improved by using CuO-water nanofluid.	[42]

Table 2 Properties of nanoparticles

	Molecular formula	Purity/%	Particle size/nm	Density/kg m ⁻³	Phase	Color	Surface area/m ² g ⁻¹
Aluminum Oxide	Al ₂ O ₃	99.5	78	4000	Gamma	White	20
Titanium Dioxide	TiO ₂	99.5	38	4230	Anatase	White	55

Table 3 Characteristics of TEC1-12706 [46]

Hot surface temperature	Q _{max} / Watt	ΔT _{max} / °C	I _{max} / Ampere	V _{max} / Volt	Module resistance / Ohm
25 °C	71	66	8.5	15.4	1.5
50 °C	79	75	8.4	17.5	1.8

energy required by the vaccine cabinet during the day can be met from solar energy. In addition, in cases where there is no power supply, the refrigerant can be circulated with the electricity provided by the battery in the cabin. In the TEC mechanism placed on the side surface of the vaccine cabinet, aluminum fins and fans were used on the cold side of the Peltier. On the hot side, a liquid-cooled block and aluminum fins integrated into this block are used. Water and nanofluid were used separately as refrigerants, and their performances were observed. Al₂O₃-TiO₂-Water hybrid nanofluid was used as a nanofluid. The thermophysical properties of nanoparticles are shown in Table 2. The results obtained from the previous study were effective in the selection of this nanofluid [35]. The nanofluids were prepared in the laboratory using a two-step method [44, 45].

A single-stage Peltier (TEC1-12706) was used in the system. Specific features of the Peltier used are shown in Table 3 [46].

A 12 V (Volt) 1.5 A (Ampere) circulation pump was used to circulate the refrigerant in the system. Additionally,

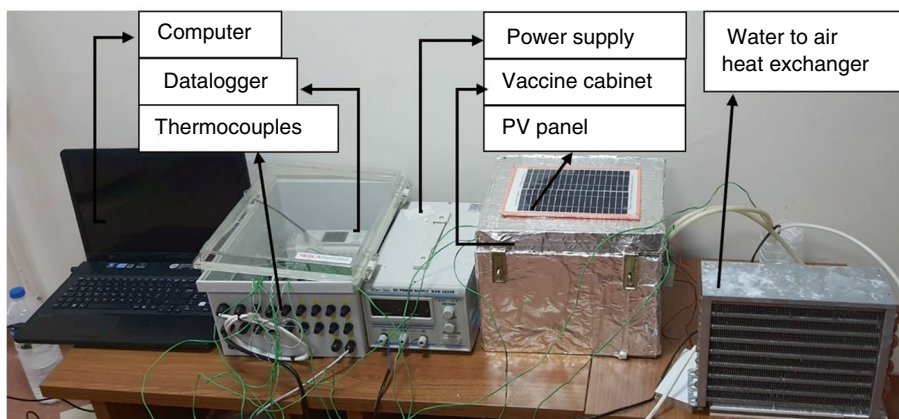
a water-to-air exchanger and fan were used to cool the heated fluid again.

Method

The TEC mechanism is placed on the side of the vaccine cabinet. In the mechanism, an aluminum heatsink was used on the cold side of the Peltier. First, a liquid-cooled block was used on the hot surface, followed by an aluminum heatsink. The refrigerant fluid, which sweeps the heat from the hot surface of the Peltier, is sent to the water-to-air heat exchanger. Here, the fluid that releases its heat goes to the mini fluid pool, and from there, it is sent back to the cooling block with the help of a circulation pump. The established experimental setup is shown in Fig. 3.

K-type thermocouples were used to measure vaccine cabinet temperature, cold and hot surface temperatures, vaccine temperature, refrigerant temperature and outdoor temperature. The experiments were carried out at two different outdoor temperatures. Separate tests were carried out using water without nanoparticle addition and Al₂O₃-TiO₂-Water nanofluid as the refrigerant. In addition, the use and non-use of a fan in the heat exchanger section were tested separately. During the experiments, the test period and the stabilization time of the system were considered.

Two main equations are used to determine the performance data of the vaccine cabinet: The first of these equations, Cooling power (Q_c), is calculated according to the equation below [47].

Fig. 3 Experimental setup

$$Q_c = (|\alpha_n| + |\alpha_p|)T_c I - 1/(2)I^2(R_e + R_t) - k(T_h - T_c) \quad (1)$$

α represents the Seebeck coefficients, the indices n and p represent pairs of n- and p-type elements, R is the electrical resistance, and the indices e and t represent electrodes and thermocouples. T is the temperature, and the indices c and h indicate the cold and hot sides, respectively. I in the equation is the current.

The COP value is calculated by the ratio of Q_c to the total electrical load.

$$COP = \frac{Q_c}{P_e} \quad (2)$$

The P_e is electrical power.

Uncertainty analysis

During experimental studies, small errors may occur, whether predictable or unpredictable, due to both the person performing the experiment and the devices and equipment used. The reasons for these errors may arise from unstable environmental conditions, uncalibrated devices and operating sensitivities of the equipment. Uncertainty analysis is a methodological approach used to determine the sensitivity of the results in determining these errors [48].

The total uncertainty for n independent variables is calculated according to the formula [49];

$$W_Q = \left[\left(\frac{\partial Q}{\partial X_1} \times W_1 \right)^2 + \left(\frac{\partial Q}{\partial X_2} \times W_2 \right)^2 + \left(\frac{\partial Q}{\partial X_n} \times W_n \right)^2 \right]^{1/2} \quad (3)$$

Here, Q, X and W are the dimensions to be measured, the variable affecting the measurement and the independent variable, respectively.

The uncertainties of thermocouples used, voltages, and currents are $\pm 0.05^\circ\text{C}$, $\pm 0.1\text{ V}$, and $\pm 0.1\text{ A}$, respectively.

The Seebeck coefficient:

$$\left(|\alpha_n| + |\alpha_p| \right) = \frac{V_{\max}}{T_h} = 0.05 \quad (4)$$

V_{\max} is the maximum voltage. During the experiments, 9V voltage was applied to the system and it was observed that it drew 6A current.

For the situation under uncertainty analysis;

$T_h = 15^\circ\text{C}$, $T_c = -4^\circ\text{C}$, $R = 0.8$, $k = 1.28$ and Q_c is calculated to be 61.025 W.

$$\frac{\partial Q_c}{\partial T_c} = \left(|\alpha_n| + |\alpha_p| \right) I + k = 0.05(6) + 1.28 = 1.58 \quad (5)$$

$$\frac{\partial Q_c}{\partial I} = \left(|\alpha_n| + |\alpha_p| \right) T_c - I(R_e + R_t) = 0.05(-4) - (6)(0.8) = -5 \quad (6)$$

$$\frac{\partial Q_c}{\partial T_h} = -k = -1.28 \quad (7)$$

$$W_{Q_c} = \left[\left(\frac{\partial Q_c}{\partial T_c} \times 0.05 \right)^2 + \left(\frac{\partial Q_c}{\partial I} \times 0.1 \right)^2 + \left(\frac{\partial Q_c}{\partial T_h} \times 0.05 \right)^2 \right]^{1/2} \quad (8)$$

$$= [(1.58 \times 0.05)^2 + (-5 \times 0.1)^2 + (-1.28 \times 0.05)^2]^{1/2} = 0.51$$

$$\frac{W_{Q_c}}{Q_c} = \frac{0.51}{61.025} \times 100 = \%0.83 \quad (9)$$

$$P_e = V \times I = 9 \times (6) = 54\text{ W} \quad (10)$$

$$\frac{\partial P_e}{\partial V} = I = 6 \quad (11)$$

$$\frac{\partial P_e}{\partial I} = V = 9 \quad (12)$$

$$W_{P_e} = \left[\left(\frac{\partial P_e}{\partial V} \times 0.1 \right)^2 + \left(\frac{\partial P_e}{\partial I} \times 0.1 \right)^2 \right]^{1/2} \quad (13)$$

$$= [(6 \times 0.1)^2 + (9 \times 0.1)^2]^{1/2} = 1.08$$

$$\frac{W_{P_e}}{P_e} = \frac{1.08}{54} \times 100 = \%2 \quad (14)$$

$$COP = \frac{Q_c}{P_e} = \frac{61.025}{54 + 32} = 0.71 \quad (15)$$

$$\frac{\partial COP}{\partial Q_c} = \frac{1}{P_e} = \frac{1}{86} = 0.011 \quad (16)$$

$$\frac{\partial COP}{\partial P_e} = -\frac{Q_c}{P_e^2} = -\frac{61.025}{(86)^2} = -0.0082 \quad (17)$$

$$W_{COP} = \left[\left(\frac{\partial COP}{\partial Q_c} \times 0.51 \right)^2 + \left(\frac{\partial COP}{\partial P_e} \times 1.08 \right)^2 \right]^{1/2} \quad (18)$$

$$= [(0.011 \times 0.51)^2 + (-0.0082 \times 1.08)^2]^{1/2} = 0.01$$

$$\frac{W_{COP}}{COP} \times 100 = \%1.4 \quad (19)$$

The total uncertainty has been calculated as %1.4 for the worst case.

Results

The experiments were carried out in two different ambient temperatures: 13 °C and 26 °C. For both outdoor temperatures, cases using water as the coolant and using $\text{Al}_2\text{O}_3\text{-TiO}_2\text{-Water}$ hybrid nanofluid were observed. In addition, during the experiments, the use and non-use of fans in the water-to-air heat exchanger were examined separately. Before the results obtained from the study are presented, each situation is named as in Table 4 for the sake of understandability of the results and the situations examined.

For Case 1, it was observed that at the end of 1470 seconds, the temperature of the vaccine cabinet decreased from 13.2 to 5.3 °C. At the end of the same period, it was observed that the temperature of the vaccine in the vaccine cabinet reached the vaccine storage conditions. In this case,

Table 4 Conditions under which the experiments were performed

	Ambient temp./°C	Refrigerant	Fan
Case 1	13	Water	Without fan
Case 2	13	Water	With fan
Case 3	13	$\text{Al}_2\text{O}_3\text{-TiO}_2\text{-Water}$	Without fan
Case 4	13	$\text{Al}_2\text{O}_3\text{-TiO}_2\text{-Water}$	With fan
Case 5	26	Water	Without fan
Case 6	26	Water	With fan
Case 7	26	$\text{Al}_2\text{O}_3\text{-TiO}_2\text{-Water}$	Without fan
Case 8	26	$\text{Al}_2\text{O}_3\text{-TiO}_2\text{-Water}$	With fan

the average COP value of the system is calculated as 1.18. The measured temperature values for Case 1 are shown in Fig. 4a, and the COP curve is shown in Fig. 4b.

For Case 2, it was observed that at the end of 1470 seconds, the temperature of the vaccine cabinet decreased from 13.3 to 2 °C. It was observed that the temperature of the vaccine in the vaccine cabinet reached the vaccine storage conditions faster than Case 1 with the effect of using a fan. In addition, a decrease in the COP value of the system was observed as the temperature difference between the hot and cold surfaces of the TEC increased. From the definition of cooling power, the Fourier effect, that is, the temperature difference, is the most effective parameter on the Peltier performance. Because no significant change in electrical resistance is observed within Peltier's operating temperature ranges. Therefore, it is expected that when the temperature difference between the surfaces of the Peltier increases, the COP value of the system will decrease. The measured temperature values for Case 2 are shown in Fig. 5a, and the COP curve is shown in Fig. 5b.

For Case 3, when nanofluid was used as a coolant, it was observed that the temperature of the vaccine cabinet decreased from 13.3 to 5.1 °C at the end of 1470 seconds. At the end of the same period, it was observed that the temperature of the vaccine in the vaccine cabinet reached the vaccine storage conditions. In this case, the average COP value of the system is calculated as 1.19. The measured temperature values for Case 3 are shown in Fig. 6a, and the COP curve is shown in Fig. 6b.

For case 4, it was observed that at the end of 1470 seconds, the temperature of the vaccine cabinet decreased from 13.8 to 0.6 °C. It was observed that the temperature of the vaccine in the vaccine cabinet reached the vaccine storage conditions faster than in Case 3 with the effect of

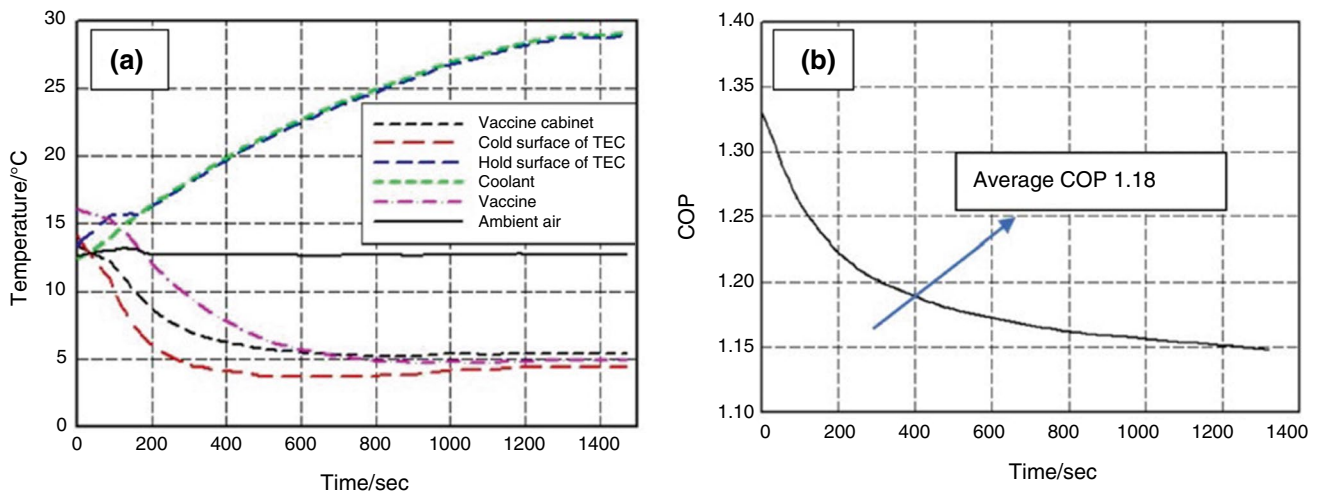


Fig. 4 Experimental results for Case 1 (A) and COP curves for Case 1 (B)

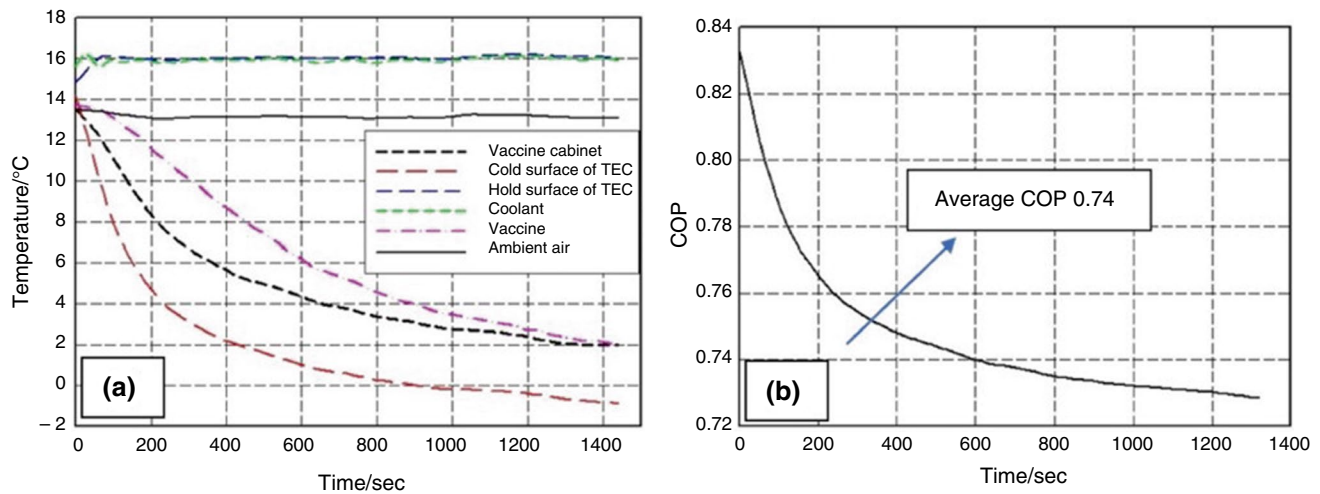


Fig. 5 Experimental results for Case 2 (A) and COP curves for Case 2 (B)

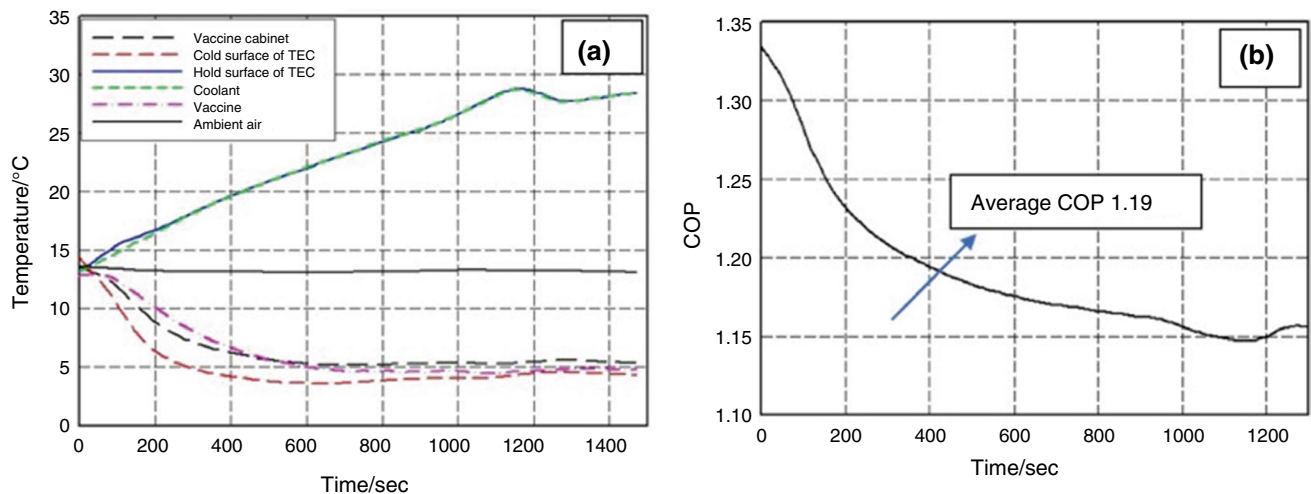


Fig. 6 Experimental results for Case 3 (A) and COP curves for Case 3 (B)

using a fan. In addition, a decrease in the COP value of the system was observed as the temperature difference between the hot and cold surfaces of the TEC increased. The measured temperature values for Case 4 are shown in Fig. 7a, and the COP curve is shown in Fig. 7b.

In the tests carried out in 26 °C outdoor conditions, the time for the system to reach equilibrium was observed to be 1200 seconds. For Case 5, it was observed that the vaccine cabinet temperature decreased from 23.5 to 12.6 °C at the end of 1200 s. It was observed that under the conditions determined for Case 5, the cabinet temperature could not reach the vaccine storage temperature. Additionally, in this case, the average COP value of the system was observed to be 1.15. The measured temperature values for Case 5 are shown in Fig. 8a, and the COP curve is shown in Fig. 8b.

For Case 6, it was observed that the temperature of the vaccine cabin decreased from 22 to 10.1 °C at the end of 1200 s. Additionally, in this case, it was observed that the average COP value of the system was 0.78. The measured temperature values for Case 5 are shown in Fig. 9a, and the COP curve is shown in Fig. 9b.

For Case 7, when nanofluid was used as a coolant, it was observed that the temperature of the vaccine cabinet decreased from 23.8 to 12 °C at the end of 1200 seconds. At the end of the same period, it was observed that the temperature of the vaccine in the vaccine cabinet had not reached the vaccine storage conditions. In this case, the average COP value of the system is calculated as 1.12. The measured temperature values for Case 7 are shown in Fig. 10a, and the COP curve is shown in Fig. 10b.

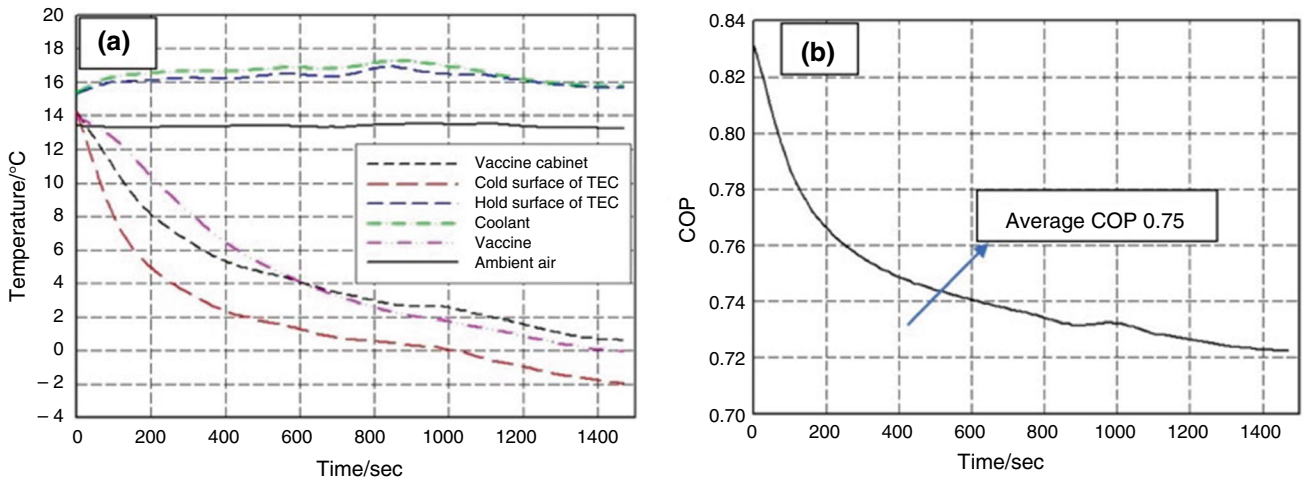


Fig. 7 Experimental results for Case 4 (A) and COP curves for Case 4 (B)

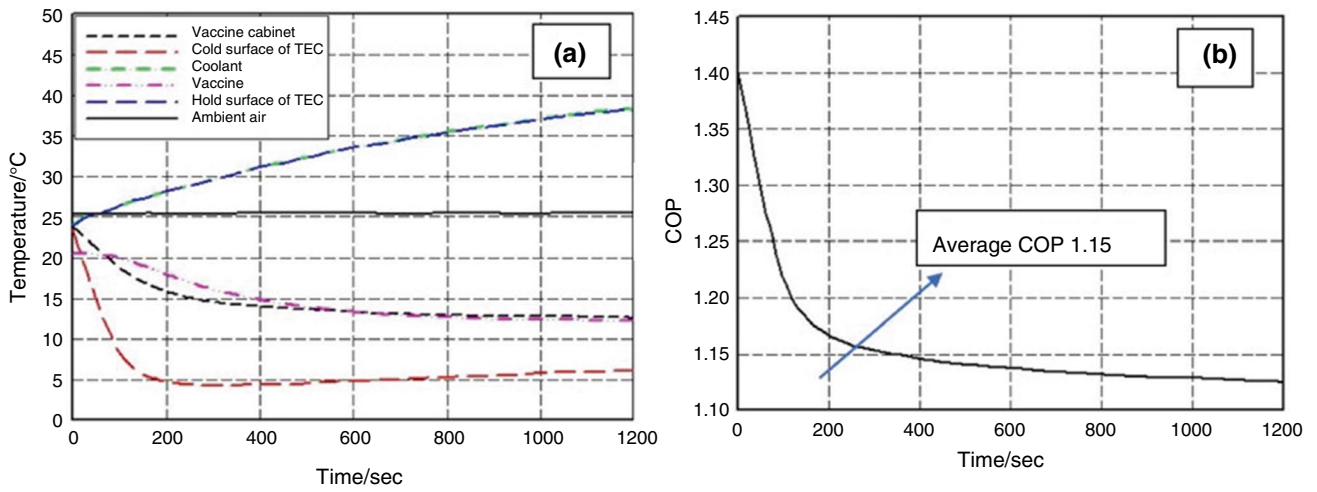


Fig. 8 Experimental results for Case 5 (A) and COP curves for Case 5 (B)

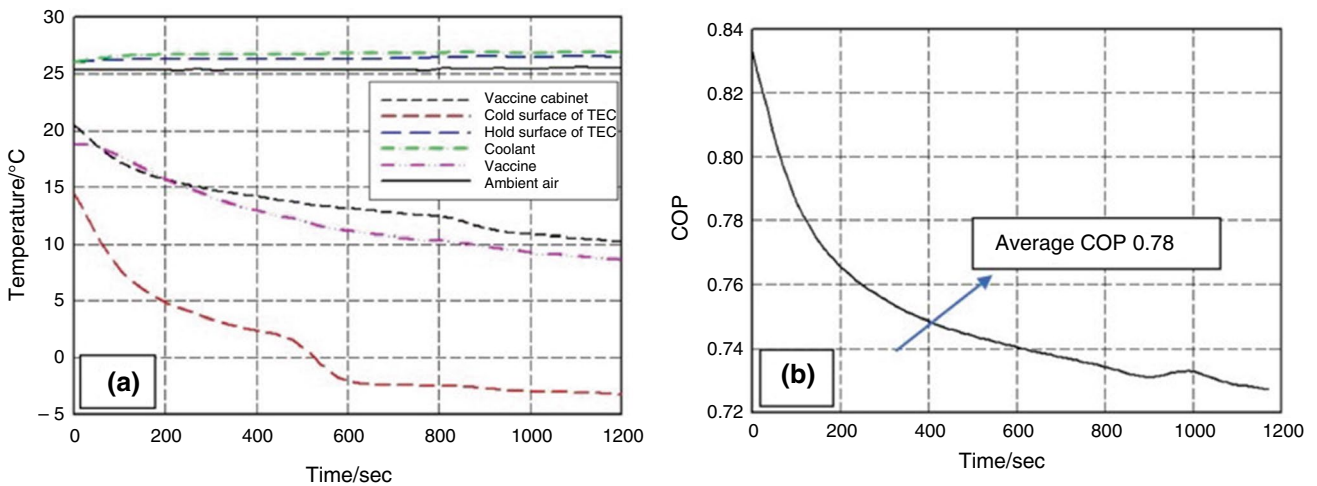


Fig. 9 Experimental results for Case 6 (A) and COP curves for Case 6 (B)

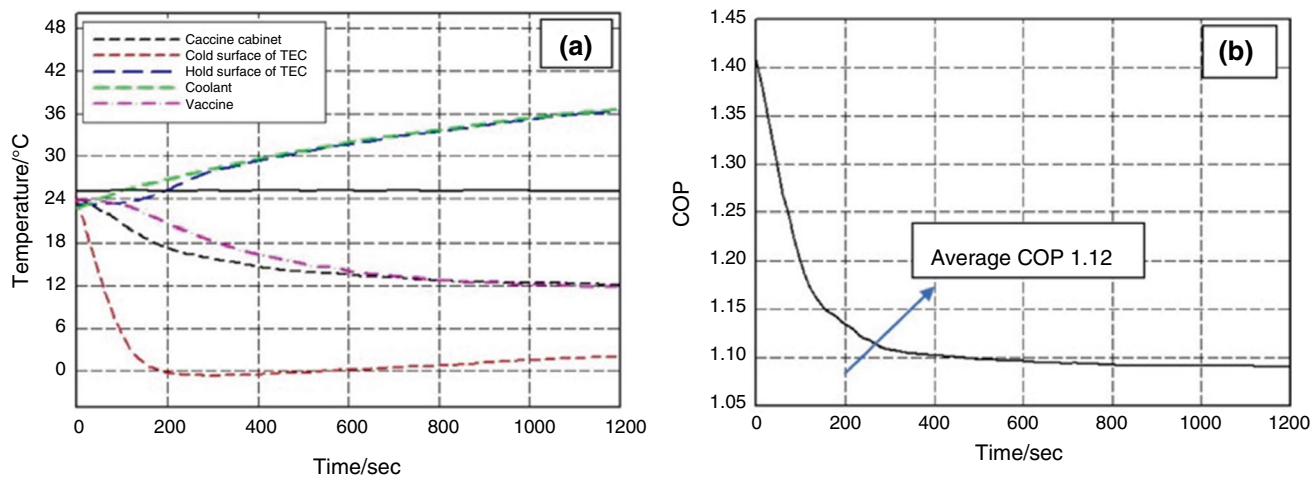


Fig. 10 Experimental results for Case 7 (A) and COP curves for Case 7 (B)

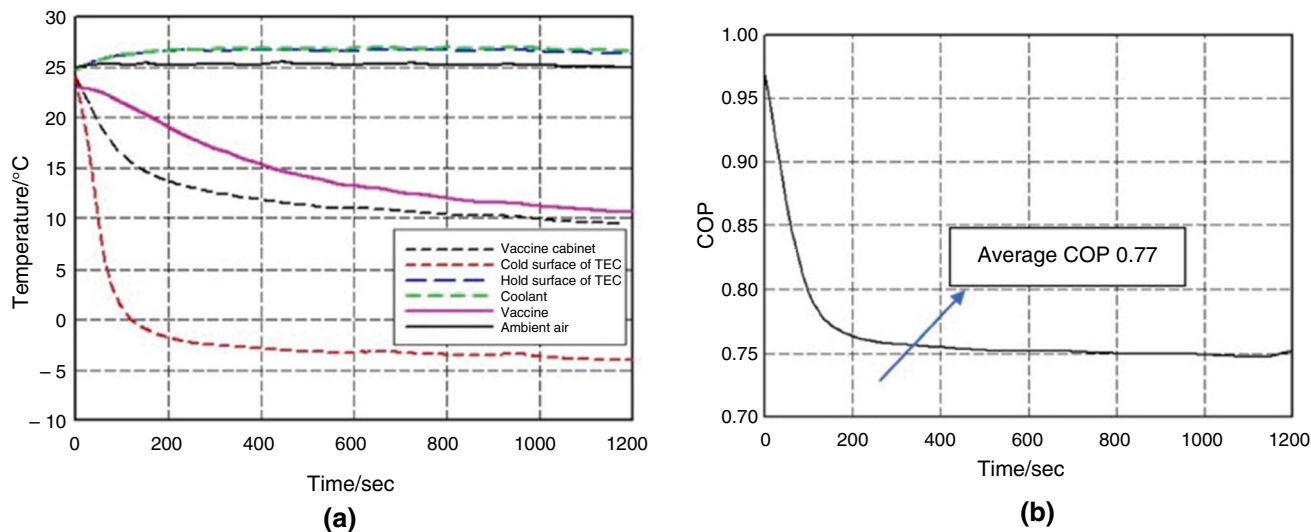


Fig. 11 Experimental results for Case 8 (A) and COP curves for Case 8 (B)

For Case 8, it was observed that at the end of 1200 seconds, the temperature of the vaccine cabinet decreased from 24.3 to 9.4 °C. In addition, a decrease in the COP value of the system was observed as the temperature difference between the hot and cold surfaces of the TEC increased. The measured temperature values for Case 8 are shown in Fig. 11a, and the COP curve is shown in Fig. 11b.

Conclusions

This study is about the design, production and performance analysis of a nanofluid-added, PV-integrated thermoelectric vaccine cabinet. Cooling performance and COP values were observed in the study carried out using different outdoor temperatures and different refrigerants. In all experiments

carried out under 13 °C outdoor conditions, vaccine temperatures reached vaccine storage conditions. Therefore, there is no need to use an extra fan in the water-to-air heat exchanger to take the heat of the refrigerant under low outdoor environmental conditions. This reduces energy consumption. In addition, in cases where nanofluid is used as a refrigerant, vaccine cabinet temperatures drop to the desired values sooner. Therefore, energy efficiency increases when nanofluids are used. In experiments carried out under 26 °C outdoor conditions, vaccine temperatures could not be reduced to the desired values. However, under these conditions, better results were obtained when nanofluids were used. It is predicted that if the cabinet insulation thickness is optimized, the desired temperatures can be reached with nanofluid even at high external temperatures. In addition, thanks to the PV panel placed on the cabinet, part of the

required electrical energy can be provided from renewable energy sources. The designed system provides significant advantages as an energy-efficient design, especially for applications that do not operate continuously and require transportation of vaccines over short and medium distances.

Declarations

Conflict of interest The authors declare that they have no known competing financial interests or personal relationships that could have appeared to influence the work reported in this paper.

Open Access This article is licensed under a Creative Commons Attribution 4.0 International License, which permits use, sharing, adaptation, distribution and reproduction in any medium or format, as long as you give appropriate credit to the original author(s) and the source, provide a link to the Creative Commons licence, and indicate if changes were made. The images or other third party material in this article are included in the article's Creative Commons licence, unless indicated otherwise in a credit line to the material. If material is not included in the article's Creative Commons licence and your intended use is not permitted by statutory regulation or exceeds the permitted use, you will need to obtain permission directly from the copyright holder. To view a copy of this licence, visit <http://creativecommons.org/licenses/by/4.0/>.

References

- Rodrigues CMC, Plotkin SA. Impact of vaccines; health, economic and social perspectives. *Front Microbiol.* 2020;11:550510.
- Ohara B, Sitar R, Soares J, Novisoff P, Nunez-Perez A, Lee H. Optimization strategies for a portable thermoelectric vaccine refrigeration system in developing communities. *J Electron Mater.* 2015;44:1614–26. <https://doi.org/10.1007/s11664-014-3491-9>.
- Bartsch SM, O'Shea KJ, Ferguson MC, Bottazzi ME, Wedlock PT, Strych U, et al. Vaccine efficacy needed for a COVID-19 coronavirus vaccine to prevent or stop an epidemic as the sole intervention. *Am J Prev Med.* 2020;59:493–503.
- Reid E, Barks J, Morrison C, Ung A, Patel R, Rebarker C, et al. Design and testing of a thermoelectrically-cooled portable vaccine cooler, 2018.
- Ay M, Akdoğan B, Fidan EM, Özbakir L, Bölümü EM, Fakültesi M, et al. Yerleştirme-rotalama problemi için iki aşamalı bir model: Covid-19 aşılmasının dağıtımı. *Pamukkale University Journal of Engineering Sciences [Internet].* 2022 [cited 2023 Dec 24];28:559–68. Available from: <https://dergipark.org.tr/en/pub/pajes/issue/72381/1168716>
- Weltermann BM, Markic M, Thielmann A, Gesenhues S, Hermann M. Vaccination management and vaccination errors: a representative online-survey among primary care physicians. *PLoS One.* 2014;9:e105119. <https://doi.org/10.1371/journal.pone.0105119>.
- Vangroenweghe F. Good vaccination practice: it all starts with a good vaccine storage temperature. *Porcine Health Manag.* 2017;3:1–7. <https://doi.org/10.1186/s40813-017-0071-4>.
- Kartoglu U, Milstien J. Tools and approaches to ensure quality of vaccines throughout the cold chain. *Expert Rev Vaccines.* 2014;13:843–54. <https://doi.org/10.1586/14760584.2014.923761>.
- Zaferani SH, Sams MW, Ghomashchi R, Chen ZG. Thermoelectric coolers as thermal management systems for medical applications: design, optimization, and advancement. *Nano Energy.* 2021;90:106572.
- Shi X-L, Zou J, Chen Z-G. Advanced thermoelectric design: from materials and structures to devices. *Chem Rev.* 2020;120:7399–515.
- Lin L, Zhang YF, Liu HB, Meng JH, Chen WH, Wang XD. A new configuration design of thermoelectric cooler driven by thermoelectric generator. *Appl Therm Eng.* 2019;160:114087.
- Pourkiaei SM, Ahmadi MH, Sadeghzadeh M, Moosavi S, Pourfayaz F, Chen L, et al. Thermoelectric cooler and thermoelectric generator devices: a review of present and potential applications, modeling and materials. *Energy.* 2019;186:115849.
- Cuce PM, Guclu T, Cuce E. Design, modelling, environmental, economic and performance analysis of parabolic trough solar collector (PTC) based cogeneration systems assisted by thermoelectric generators (TEGs). *Sustain Energy Technol Assess.* 2024;64:103745.
- Guclu T, Cuce E. Thermoelectric coolers (TECs): from theory to practice. *J Electron Mater.* 2019;48:211–30. <https://doi.org/10.1007/s11664-018-6753-0>.
- Salah WA, Abuhelwa M. Review of thermoelectric cooling devices recent applications. *J Eng Sci Technol.* 2020;15:455–76.
- Afshari F. Experimental and numerical investigation on thermoelectric coolers for comparing air-to-water to air-to-air refrigerators. *J Therm Anal Calorim.* 2021;144:855–68. <https://doi.org/10.1007/s10973-020-09500-6>.
- Chen WY, Shi XL, Zou J, Chen ZG. Thermoelectric coolers: progress, challenges, and opportunities. *Small Methods.* 2022;6:2101235. <https://doi.org/10.1002/smt.202101235>.
- Rahman MA, Widyatama A, Majid AI, Suhanan S. Peltier thermoelectric refrigeration system as the future cold storage system for indonesia: A review. *Proceedings–2019 5th International Conference on Science and Technology, ICST 2019.* 2019;
- Gao YW, Lv H, Wang XD, Yan WM. Enhanced Peltier cooling of two-stage thermoelectric cooler via pulse currents. *Int J Heat Mass Transf.* 2017;114:656–63.
- Mardini-Bovea J, Torres GA, De-la-Hoz-Franco E, Niño-Moreno J, Sabau M, Pacheco-Torres PJ. A review to refrigeration with thermoelectric energy based on the Peltier effect. *Dyna (Medellin).* 2019;86:9–18.
- Zhao D, Tan G. A review of thermoelectric cooling: Materials, modeling and applications. *Appl Therm Eng.* 2014;66:15–24.
- Abdul-Wahab SA, Elkamel A, Al-Damkhi AM, Al-Habsi IA, Al-Rubai'ey' HS, Al-Battashi AK, et al. Design and experimental investigation of portable solar thermoelectric refrigerator. *Renew Energy.* 2009;34:30–4.
- Min G, Rowe DM. Experimental evaluation of prototype thermoelectric domestic-refrigerators. *Appl Energy.* 2006;83:133–52.
- Wiriyasart S, Hommalee C, Prurapark R, Srichat A, Naphon P. Thermal efficiency enhancement of thermoelectric module system for cold-hot water dispenser; Phase II. *Case Stud Thermal Eng.* 2019;15:100520.
- Tawfik MM. Experimental studies of nanofluid thermal conductivity enhancement and applications: a review. *Renew Sustain Energy Rev.* 2017;75:1239–53.
- Huang HS, Weng YC, Chang YW, Chen SL, Ke MT. Thermoelectric water-cooling device applied to electronic equipment. *Int Commun Heat Mass Trans.* 2010;37:140–6.
- Hu HM, Ge TS, Dai YJ, Wang RZ. Experimental study on water-cooled thermoelectric cooler for CPU under severe environment. *Int J Refrige.* 2016;62:30–8.
- Gökçek M, Şahin F. Experimental performance investigation of minichannel water cooled-thermoelectric refrigerator. *Case Stud Thermal Eng.* 2017;10:54–62.

29. KILIÇ M. Elektronik Sistemlerin Soğutulmasında Nanoakışkanlar ve Çarpın Jetlerin Müşterek Etkisinin İncelenmesi. Çukurova Üniversitesi Mühendislik-Mimarlık Fakültesi Dergisi, 33:121–32, 2018. Available from: <https://dergipark.org.tr/en/pub/cukurovaummfd/issue/42374/500597>
30. Nguyen CT, Roy G, Gauthier C, Galanis N. Heat transfer enhancement using Al_2O_3 -water nanofluid for an electronic liquid cooling system. Appl Therm Eng. 2007;27:1501–6.
31. Özeriç S, Kakaç S, Yazıcıoğlu AG. Enhanced thermal conductivity of nanofluids: a state-of-the-art review. Microfluid Nanofluidics. 2010;8:145–70. <https://doi.org/10.1007/s10404-009-0524-4>.
32. Yu W, France DM, Routbort JL, Choi SUS. Review and comparison of nanofluid thermal conductivity and heat transfer enhancements. Heat Trans Eng. 2008;29:432–60. <https://doi.org/10.1080/01457630701850851>.
33. Cuce E, Cuce PM, Guclu T, Besir AB. On the use of nanofluids in solar energy applications. J Thermal Sci. 2020;29:513–34. <https://doi.org/10.1007/s11630-020-1269-3>.
34. Cuce E, Guclu T, Cuce PM. Improving thermal performance of thermoelectric coolers (TECs) through a nanofluid driven water to air heat exchanger design: An experimental research. Energy Convers Manag. 2020;214: 112893.
35. Cuce PM, Cuce E, Guclu T, Shaik S, Alshahrani S, Ahamed Saleel C. Effect of using hybrid nanofluids as a coolant on the thermal performance of portable thermoelectric refrigerators. Sustain Energy Technol Assess. 2022;53: 102685.
36. Cuce PM, Guclu T, Cuce E. The effect of nanofluid usage on electricity consumption in thermoelectric refrigeration application: an experimental study. Gazi J Eng Sci. 2022;8:228–36.
37. Wiriyaart S, Suksusron P, Hommalee C, Siricharoenpanich A, Naphon P. Heat transfer enhancement of thermoelectric cooling module with nanofluid and ferrofluid as base fluids. Case Stud Thermal Eng. 2021;24: 100877.
38. Putra N, Iskandar FN. Application of nanofluids to a heat pipe liquid-block and the thermoelectric cooling of electronic equipment. Exp Therm Fluid Sci. 2011;35:1274–81.
39. Ahammed N, Asirvatham LG, Wongwises S. Thermoelectric cooling of electronic devices with nanofluid in a multiport minichannel heat exchanger. Exp Therm Fluid Sci. 2016;74:81–90.
40. Mandev E, Muratçobanoğlu B, Manay E, Şahin B, Teimuri-Mofrad R, Rahimpour S, et al. Performance analysis of thermoelectric cooling systems equipped with surface-modified and recycled nanofluids. J Enhanced Heat Trans. 2023;30:33–50.
41. Agwu Nnanna AG, Rutherford W, Elomar W, Sankowski B. Assessment of thermoelectric module with nanofluid heat exchanger. In: Heat Transfer, fluid flows, and thermal systems, parts A and B. ASMEEDC; 2007. Volume 8, p. 663–72.
42. Afzal A, Samee M, Razak A. Experimental thermal investigation of CuO-W nanofluid in circular minichannel. Model Meas Control B. 2017;86:335–44.
43. A700000009609792.pdf [Internet]. Available from: <https://docs.rs-online.com/cf70/A700000009609792.pdf>
44. Sidik NAC, Mohammed HA, Alawi OA, Samion S. A review on preparation methods and challenges of nanofluids. Int Commun Heat Mass Trans. 2014;54:115–25.
45. Ghadimi A, Saidur R, Metselaar HSC. A review of nanofluid stability properties and characterization in stationary conditions. Int J Heat Mass Transf. 2011;54:4051–68.
46. URL-2 [Internet]. [cited 2023 Dec 26]. Available from: <https://pdf1.alldatasheet.com/datasheet-pdf/download/227421/ETC2/TEC1-12708.html>
47. Zhu W, Deng Y, Wang Y, Wang A. Finite element analysis of miniature thermoelectric coolers with high cooling performance and short response time. Microelectron J. 2013;44:860–8.
48. Tian W, Heo Y, de Wilde P, Li Z, Yan D, Park CS, et al. A review of uncertainty analysis in building energy assessment. Renew Sustain Energy Rev. 2018;93:285–301.
49. Coleman HW, Glenn SW. Uncertainty analysis. In: Johnson R, editor. Handbook of fluid dynamics. NJ: CRC Press; 2016. p. 51.1–51.5.

Publisher's Note Springer Nature remains neutral with regard to jurisdictional claims in published maps and institutional affiliations.